Adipocyte

ISSN: (Print) (Online) Journal homepage: www.tandfonline.com/journals/kadi20

Adipogenic characterization of immortalized CD55^{+} progenitor cells from human white adipose tissue

Morgane Couchet, Hui Gao, Felix Klingelhuber, Jutta Jalkanen, Thais De Castro Barbosa, Muhmmad Omar-Hmeadi, Lucas Massier, Natalie Krahmer, Niklas Mejhert & Mikael Rydén

To cite this article: Morgane Couchet, Hui Gao, Felix Klingelhuber, Jutta Jalkanen, Thais De Castro Barbosa, Muhmmad Omar-Hmeadi, Lucas Massier, Natalie Krahmer, Niklas Mejhert & Mikael Rydén (20 Nov 2023): Adipogenic characterization of immortalized CD55^{+} progenitor cells from human white adipose tissue, Adipocyte, DOI: 10.1080/21623945.2023.2283213

To link to this article: https://doi.org/10.1080/21623945.2023.2283213

Publisher: Taylor & Francis & Informa UK Limited, trading as Taylor & Francis Group

Journal: *Adipocyte*

DOI: 10.1080/21623945.2023.2283213

Adipogenic characterization of immortalized CD55^{+} progenitor cells from human white adipose tissue

Morgane Couchet[1], Hui Gao[2], Felix Klingelhuber[3], Jutta Jalkanen[1], Thais De Castro Barbosa[1], Muhmmad Omar-Hmeadi[1], Lucas Massier[1], Natalie Krahmer[3], Niklas Mejhert[1,4*], Mikael Rydén[1,4*]

[1] Department of Medicine (H7), Karolinska Institutet, 141 86 Stockholm, Sweden.

[2] Department of Biosciences and Nutrition, Karolinska Institutet, 141 86 Stockholm, Sweden.

[3] Institute for Diabetes and Obesity, Helmholtz Zentrum München, 85764 Neuherberg, Germany; German Center for Diabetes Research, Neuherberg, Germany.

[4] These authors contributed equally

* Correspondence: niklas.mejhert@ki.se and mikael.ryden@ki.se

ABSTRACT

Background: Mature adipocytes are notoriously difficult to study *ex vivo* and alternative cell culture systems have therefore been developed. One of the most common models are human adipose progenitor cells (hAPCs). Unfortunately, these display replicative senescence after prolonged culture conditions, which limits their use in mechanistic studies.

Methods: Herein, we knocked in human telomerase reverse transcriptase (TERT) into the *AAVS1* locus of $CD55^+$ hAPCs derived from abdominal subcutaneous adipose tissue and characterized the cells before and after differentiation into adipocytes.

Results: Immortalized TERT-hAPCs retained proliferative and adipogenic capacities comparable to those of early-passage wild type hAPCs for >80 passages. In line with this, our integrative transcriptomic and proteomic analyses revealed that TERT-hAPCs displayed robust adipocyte expression profiles in comparison to wild type hAPCs. This was confirmed by functional analyses of lipid turnover where TERT-hAPCs exhibited pronounced responses to insulin and pro-lipolytic stimuli such as isoprenaline, dibutyrul cAMP and tumor necrosis factor alpha. In addition, TERT-hAPCs could be readily cultured in both standard 2D and 3D-cultures and proteomic analyses revealed that the spheroid culture conditions improved adipogenesis.

Conclusion: Through descriptive and functional studies, we demonstrate that immortalization of human $CD55^+$ hAPCs is feasible and results in cells with stable proliferative and adipogenic capacities over multiple passages. As these cells are cryopreservable, they provide the additional advantage over primary cells of allowing repeated studies in both 2D and 3D model systems with the same genetic background. (234/250)

INTRODUCTION

Perturbed white adipocyte function, e.g., alterations in the capacity to store and release lipids, is associated with multiple cardiometabolic complications (1). To obtain causal insights into these relationships, mechanistic studies of donor-derived fat cells are required. Unfortunately, the buoyancy and fragility of isolated mature fat cells ex vivo limits these analyses. Multiple efforts have therefore been made to create alternative in vitro models (2,3). Virtually all of these are based on different types of progenitor cells, which are induced to differentiate following the addition of specific pro-adipogenic cocktails. While most of the models are grown in standard 2D cultures, we and others have recently demonstrated that differentiating the cells in organotypic 3D microenvironments results in phenotypes that closely resemble freshly isolated mature adipocytes (4–6).

A common approach to generate adipocytes in vitro is to isolate the stromal vascular fraction (SVF) of white adipose tissue. The SVF contains adipose progenitor cells (hAPCs), which respond readily to adipogenic induction. However, primary hAPCs have limited proliferative capacity and several investigators have therefore immortalized these cells by integrating telomerase reverse transcriptase (TERT) by viral transduction (7–11). A caveat with this approach is that TERT is randomly introduced into the genome, which may affect the expression of multiple genes and thereby cell function of the edited cells (8,12).

Herein, we immortalized hAPCs from a male donor by knocking-in hTERT in a safe harbor locus by CRISPR/Cas9-mediated engineering. Our characterizations, which include functional and transcriptomic/proteomic profiling, demonstrate that the edited cells retain adipogenic capacity and hormonal sensitivity/responsiveness without signs of replicative senescence for >80 passages in both 2D and 3D culture conditions.

RESULTS

Generation of immortalized hAPCs

To immortalize hAPCs, we knocked in the EF-1 alpha promoter driving the expression of Puromycin N-acetyltransferase-P2A-hTERT in the *AAVS1* safe harbor locus (also known as *PPP1R12C*) by CRISPR/Cas9-mediated engineering (**Figure 1A**). For this, we electroporated a repair template together with a bicistronic vector expressing the AAVS1-T2 targeting guide RNA as well as Cas9-T2A-EGFP. GFP^+ cells were selected using fluorescence-activated cell sorting (FACS) and subsequently cultured in puromycin-containing media (**Figure 1B**). We opted to use this double selection to increase the proportion of edited cells. To confirm successful genome integration, we analyzed the mRNA expression of *TERT* and the gene encoding Puromycin N-acetyltransferase (*pac*) in edited and non-edited hAPCs. Our results showed qPCR-detectable expression of these two genes only in edited cells (**Figure 1C**). These findings were confirmed by western blot, where TERT protein expression was barely detectable in non-edited, wild type (WT) cells compared to immortalized hAPCs (**Figure 1D**). We named these immortalized cells TERT-hAPCs and refer to non-edited cells henceforth as WT-hAPCs.

We next determined the proliferative capacity of TERT-hAPCs and WT-hAPCs by counting the cumulative number of cells over multiple passages (**Figure 1E**). As expected, WT-hAPCs, counted from passage 15 to passage 40, showed signs of replicative senescence after approximately 30-35 passages. In contrast, TERT-hAPCs displayed a consistent increase in cell number between passage 28 to 80 with no obvious change in cell morphology over time compared to WT-hAPCs (**Figure 1F**). These assessments were complemented by quantifying doubling times which were significantly lower in TERT-hAPCs (on average 20.8 hours for passage 31-81) compared to WT-hAPCs (on average 25.4 hours for passage 12 to 31) (**Figure 1G**).

TERT-hAPCs remain $CD55^+$ across multiple passages

Both human and murine APCs constitute a heterogenous cell population where the subset marked by CD55 is capable of differentiating into committed preadipocytes (13,14). This is corroborated by a recent meta-analysis of single cell data, wherein $CD55^+$ cells were described as primordial adipocyte progenitors in human white adipose tissue (15). To test which type of hAPC the non-edited and edited cells represented and whether prolonged in vitro proliferation or gene editing influenced this, we performed FACS on WT-hAPCs (P13) as well as TERT-hAPCs at early (P32) and late (P83) passages (**Figure 1H**). As expected, our analyses showed that all cells were negative for leukocyte (CD45) and endothelial (CD31) cell markers. In contrast, cells were clearly positive for CD55 and remained so across passages. In concordance with previous results, the $CD55^+$ cells were negative for CD34, which is a cell stemness marker downregulated by *in vitro* culture (16,17).

TERT-hAPCs retain the capacity to differentiate into adipocytes over multiple passages

We tested the adipogenic capacity of TERT-hAPCs in standard 2D culture following induction with a pro-adipogenic cocktail. Results were compared with WT-hAPCs for up to 30-35 passages as the unedited cells underwent replicative senescence after that. As displayed in **Figure 2A-B**, we determined lipid accumulation and adiponectin secretion at the end of adipogenesis across passages. While TERT-hAPCs retained a similar degree of lipid accumulation over time, WT-hAPCs displayed fewer cells with heterogenous lipid accumulation at later passages, a phenotype which was also observed in two other available human adipocyte models (hWA (7) and ASC52telo (11), **Figures 2A and S1A-C**). Furthermore, both cell types secreted similar amounts of adiponectin and in TERT-hAPCs, these levels were unaltered up to >80 passages (**Figure 2B**). To further characterize the cells, we performed RNA-sequencing and proteomic analyses of TERT-hAPCs and WT-hAPCs as described in the Methods section. Data integration of the transcriptome and proteome profiles allowed us to identify 4700 genes, which were also detected at the protein level by mass-spectrometry. Out of these, 588 entries displayed congruent mRNA and

protein regulation (402 higher and 186 lower, false discovery rate <0.05) comparing edited vs. non-edited adipocytes. The significantly altered subsets were used as inputs to identify pathways that differed between the two hAPCs. Our results revealed that “adipogenesis” (e.g., *ACOX1*, *ALDH2*, *CD36*), “fatty acid metabolism” (e.g., *CPT2*, *GPD2*, *MGLL*) and “xenobiotic metabolism” (e.g., *AKR1C2*, *AKR1C3*, *CBR1*) were enriched in TERT-hAPCs *vs.* WT-hAPCs (**Figure 2C**, individual genes/proteins listed in **Tables S1-2**). In contrast, “epithelial-mesenchymal transition” represented by several genes encoding collagens and extracellular matrix (ECM) proteins (e.g., *COL1A1*, *COL3A1*, *COL6A3*) was lower in TERT-hAPCs (**Figure 2C)**. Altogether, this shows that TERT-hAPCs retain full capacity to differentiate into adipocytes over multiple passages with limited impact on most cellular pathways.

TERT-hAPCs differentiate into functional adipocytes

We followed-up on this mapping by concentrating our studies on two hallmark functional features of differentiated adipocytes, namely lipolysis and lipogenesis. Short-term incubation with the beta-adrenergic receptor agonist isoprenaline and the phosphodiesterase-resistant cAMP-analogue dibutyryl cAMP (dcAMP) resulted in a pronounced increase in glycerol release from both edited and non-edited adipocytes (**Figure 3A-B**). In addition to these two compounds, we also tested the effect of the cytokine TNF-α which has been shown to induce lipolysis in primary human fat cells (18). While TNF-α did not increase glycerol release in WT-hAPCs, we observed a two-fold induction in TERT-hAPCs (**Figure 3C**), which is comparable to the effects observed in primary *in vitro* differentiated adipocytes (18). To measure the responsiveness to insulin, we determined *de novo* lipogenesis in the absence/presence of insulin. This showed increased glucose incorporation into lipids upon insulin stimulation in both cell types (**Figure 3D**). To complement these investigations, we also tested the effects of insulin on lipolysis (concentration-dependent) and gene expression. Our results showed that TERT-hAPCs retained similar degrees of insulin sensitivity at early

and late passages (**Figures 3E-F and S2A-B**). Taken together, following *in vitro* differentiation, TERT-hAPCs display functional hallmarks of mature white adipocytes.

TERT-hAPCs form adipocyte spheroids

Finally, we tested the ability of TERT-hAPCs and WT-hAPCs to form spheroids by plating undifferentiated cells in ultra-low-attachment plates. Following adipogenic induction, both cells were able to differentiate into adipocyte spheroids with paucilocular lipid droplets (**Figure 4A**). We next tested the ability of isoprenaline to hydrolyze triacylglycerols and observed that both cell types responded with an increased glycerol release (**Figure 4B**). We complemented these studies by comparing the proteomic profiles of TERT-hAPCs and WT-hAPCs differentiated in 2D and 3D conditions, respectively (**Tables S3-4**). This revealed that in both cell types, spheroid cultures compared with standard 2D conditions were enriched for proteins involved in “adipogenesis” (e.g., ADIPOQ, FABP4, LPL), “oxidative phosphorylation” (e.g., DLAT, PDHB), “protein secretion” (e.g., IGF2R, ABCA1, CD63), “peroxisome” (e.g., ABCD2, MLYCD), and “cholesterol homeostasis” (e.g., EBP, FDPS, SCSD) (**Table S5**). Thus, our results align with recent data demonstrating that culturing cells in 3D results in profiles that differ extensively from the classical 2D models (4). In contrast, comparisons of TERT-hAPCs and WT-hAPCs in 3D showed only minor differences. In fact, the only pathway that differed between the two hAPCs was “epithelial mesenchymal transition” (e.g., COL6A2, COL1A1, COL6A3), where several collagens were higher in TERT-hAPCs (**Table S6**). Altogether, our data show that TERT-hAPCs can be used in both adipocyte 2D and 3D cultures.

DISCUSSION

In this report we describe the generation of immortalized CD55$^+$ hAPCs with pronounced proliferative and adipogenic capacities. By characterizing these cells, we show that they display protein secretion, lipid content and turnover as well as transcriptional and proteomic fingerprints of adipocytes following in vitro differentiation in both 2D and 3D cultures. Thus, the knock-in strategy described herein allows the establishment of an expandable cell source for CD55$^+$ hAPCs, which enables advanced in vitro studies in adipocytes derived from the same genetic background.

As extensively discussed elsewhere (19), there are several methods to immortalize cells. One common way is by stably expressing TERT using viral transduction and subsequent cell selection. This approach results in random integration, which together with potential effects of viral transduction, may influence cell function. For SVF-derived hAPCs, random TERT-integration has indeed been reported to impair adipocyte differentiation and function (8,12). In this study, we therefore capitalized on a targeted system where we integrated TERT into the *AAVS1* safe harbor locus, which has been shown to allow gene integration with limited off-target effects (20,21). In line with this, we demonstrate that the edited cells display a similar phenotype compared with non-edited cells without signs of replicative senescence. Therefore, our protocol for CRISPR/Cas9-mediated engineering of hAPCs, provides multiple advantages compared with prior approaches.

Our study is based on human CD55$^+$ cells from the abdominal subcutaneous region. Cells marked by this surface protein have been shown to reside in many different tissues and have the capacity to differentiate into multiple lineages, including adipocytes (22). This is, however, not the only progenitor subtype present in adipose tissue as recent single-cell studies based on adipose SVF have shown that several APCs exist. These include two anti-adipogenic populations termed fibroinflammatory progenitors (23,24) and adipogenesis-regulatory cells (13,14). Whether it is possible to isolate and immortalize these and other

types of APCs resident in different WAT depots is presently not known. However, if feasible, this could potentially open avenues for more advanced co-culture studies, which could improve our understanding of the interplay between different APCs and how they contribute to tissue function.

Edited and non-edited cells were analyzed by transcriptomic and proteomic profiling. This multi-omic approach allowed us to identify consistent differences between hAPCs at the mRNA and protein levels. In line with the functional analyses, we found that under both 2D and 3D culture conditions, TERT-hAPCs were similar to WT-hAPCs. Admittedly, TERT-hAPCs displayed lower levels of a limited set of ECM proteins under 2D conditions, which were higher under 3D conditions compared with non-edited cells (e.g., COL1A1, COL6A3, TGFB1, VCAN). We interpret these as minor stochastic differences with limited effects on adipocyte function.

Translational advances in metabolic research requires different human cell models. Our approach shows that $CD55^+$ hAPCs can be efficiently immortalized with limited effects on gene/protein expression and adipogenic capacity. However, the impact of introducing the TERT sequence, even in a safe harbor, remains to be fully explored and prolonged in vitro culture may induce genetic drift. Thus, the immortalization protocol may induce differences that we have not explored in the present work. Nevertheless, this model can be a valuable addition to current cell systems in the field of adipocyte research.

MATERIALS AND METHODS

Isolation and immortalization of WT-hAPCs

Subcutaneous hAPCs were isolated from a liposuction obtained from a male with a BMI of <25 kg/m^2. Ethical approval for studies of adipose tissue collected in connection with liposuctions was obtained from the regional ethics board in Stockholm. The donor was anonymous to all involved researchers and informed written consent to donate tissue was provided to the surgeon who was not involved in the immortalization and characterization of the cells. A total of 1.4 L lipoaspirate was rinsed with PBS in a large strainer and incubated with collagenase from *Clostridium histolyticum* (#C0130-5G, Sigma-Aldrich) for 40 minutes at 37° C. The mixture was shaken every ten minutes and following digestion filtered through 200 µm nylon strainers. The floating adipocytes were thereafter discarded and the stromal vascular infranatant collected and spun at 200 x *g* for 10 minutes. The resulting cell pellet containing 23.2 million viable cells was collected and plated in proliferation media (DMEM low glucose [#31885-023, Thermo Fisher Scientific] supplemented with 10% FBS [#SV30160, Hyclone], 10 mM HEPES [#15630-056, Thermo Fisher Scientific], 50 I.U./mL penicillin and 50 µg/mL streptomycin [#15140122, Thermo Fisher Scientific]). Cells were washed twice after 14 hours to remove debris and slowly adhering cells. To immortalize the cells, the EF-1 alpha promoter driving the expression of Puromycin N-acetyltransferase-P2A-TERT was stably integrated in the adeno-associated virus integration site 1 (*AAVS1*) locus (also known as the *PPP1R12C* locus). The Neon transfection system was used to electroporate cells with 1 µg of each plasmid per 1 million cells, settings: 1150 V, 30 ms, 2 pulses, Thermo Fisher Scientific. The following two plasmids were used: **i)** pSpCas9(BB)-2A-GFP [#48138, Addgene], in which the AAVS1-T2 targeting guide RNA sequence (5'-GGG GCC ACT AGG GAC AGG AT-3') was ligated in using the *option b* protocol described in Ran *et al*. (25) and **ii)** pSH-EFIRES-P-AtAFB2 [#129715, Addgene], which was digested using BglII [#R0144, NEB] and NotI [#R0189, NEB] and thereafter ligated with Puromycin N-acetyltransferase-P2A-TERT. For the insert, TERT was PCR amplified from the pBABE-puro-hTERT plasmid [#1771, Addgene] and Puromycin N-acetyltransferase-P2A sequences were

ordered as a gBlock Gene Fragment (Integrated DNA Technologies). The digested pSH-EFIRES-P-AtAFB2 backbone was isolated by gel electrophoresis, followed by gel extraction of the DNA using NucleoSpin Gel and PCR Clean-up [#740609, Macherey-Nagel], ligated using T4 DNA ligase [#M0202, NEB] and transformed into One Shot™ Stbl3™ Chemically Competent cells [#C737303, Thermo Fisher Scientific]. Two days following electroporation, GFP^+ cells were selected using BD FACSAria Fusion (BD Biosciences) and expanded. Subsequently, a second selection step was performed by incubating the cells with puromycin [2 µg/mL, #A1113803, Thermo Fisher Scientific] during three to four days. The media containing puromycin was changed every day and the selection was stopped when unedited control cells cultured in parallel wells were no longer viable.

Cell proliferation and differentiation of WT- and TERT-hAPCs

Cells were cultured at 37° C in a humidified atmosphere with 5% CO_2 in proliferation media (described above) supplemented with 2.5 ng/mL fibroblast growth factor 2 (FGF2), [#F0291, Merck]. Three days after confluence, FGF2 was removed from the media (day -1) and differentiation was induced the next day (day 0) using differentiation media composed of William´s E medium [#A1217601, Thermo Fisher Scientific] supplemented with 2 mM L-glutamine [#25030024, Thermo Fisher Scientific], 50 I.U./mL penicillin and 50 µg/mL streptomycin [#15140122, Thermo Fisher Scientific], 1x insulin (10 µg/mL), transferrin (5.5 µg/mL, selenium solution (0.0067 µg/mL) [#4140045, Thermo Fisher Scientific], 100 nM dexamethasone [#D1756, Merck], 10 µg/mL transferrin [#T8158, Merck], 500 µM 3-Isobutyl-1-methylxanthine [#I5879, Sigma-Aldrich], 10 nM cortisol [#H0396, Sigma-Aldrich], 2 nM 3,3′,5-Triiodo-L-thyronine [#T6397, Sigma-Aldrich], 10 µM rosiglitazone [#71740, Cayman Chemical], 33 µM biotin [#B4639, Sigma-Aldrich], and 17 µM pantothenic acid [#P5155, Sigma-Aldrich]. Proliferation and differentiation media were replaced every three to four days until adipocytes were fully differentiated (2D culture: day 13, 3D culture: day 17). For spheroid formation, cells were cultured in 96 wells ultra-low attachment round bottom plates [#CLS7007, Merck] as described before (4). In brief, spheroids were differentiated with all the

components present in the differentiation media until day 17, followed by six days in William´s E medium supplemented with L-glutamine, penicillin/streptomycin, 1x insulin, transferrin, selenium solution and dexamethasone. To evaluate insulin's effects on gene expression and lipolysis, the insulin concentration on differentiation day 10 was reduced 20-fold (0.25 µg/mL) and completely omitted on differentiation day 12. On the day of the experiment (day 13), the media was changed to fresh medium without insulin for three hours. Cells were then treated without or with insulin [#I9278, Sigma-Aldrich] for two or three hours for analyses of gene expression or lipolysis, respectively.

TERT-hWA and ASC52telo cultures

TERT-hWA were proliferated in Advanced DMEM/F12 [#12-634-010, Thermo Fisher Scientific] supplemented with 10% FBS, L-glutamine (2 mM), penicillin (62.5 µg/ml), streptomycin (100 µg/ml), and basic fibroblast growth factor (bFGF) (2.5 ng/ml) as previously described (7). ASC52telo (ATCC® SCRC-4000™) were proliferated in DMEM low glucose supplemented with 10% FBS, 50 I.U./mL penicillin and 50 µg/mL streptomycin as described (11) . Both cell types were differentiated in supplemented William's E medium as described above up to day 13.

Proliferation capacity and doubling times

To assess proliferation and doubling times, WT-hAPCs and TERT-hAPCs were trypsinized and equal numbers of cells were plated in proliferation media. After 12, 24, 36, 48, 72 hours of incubation, cells were collected and counted using Bürker counting chambers. Doubling times were calculated as described previously (7) using the following formula:

$$Doubling\ time\ (days) = \frac{Duration\ (days) * LOG(2)}{\big(LOG(Number\ of\ cells\ final)\big) - \big(LOG(Number\ of\ cells\ initial)\big)}$$

Flow cytometric analysis

To quantify the abundance of selected surface markers, cells were dissociated with trypsin, pelleted (200 x *g* for 10 minutes), and resuspended in washing buffer (PBS supplemented with 0.5% BSA [#A4503, Sigma-Aldrich] and 2 mM EDTA [#E7889, Sigma-Aldrich]). Subsequently, the cells were passed through a 35 µm cell strainer [#7340001, VWR], centrifuged as above, and resuspended in antibody solution containing the following fluorophore-labeled antibodies: the pan-leukocyte marker CD45-Alexa Fluor 700 [1:100, #560566, BD Biosciences], the endothelial marker CD31-Brilliant Violet 650 [1:100, #740571, BD Biosciences], as well as the progenitor markers CD34-PE-CF594 [1:100, #562449, BD Biosciences] and CD55-Brilliant Violet 786 [1:40, #742681, BD Biosciences]. Samples were incubated in dark at 4° C for 30 minutes washed, resuspended in FACS buffer (PBS supplemented with 0.1% BSA and 2 mM EDTA) and filtered through a 35 µm cell strainer. Dead cells were excluded using the 7AAD-dye [1:10 000, #559925, BD Biosciences], which was added to the samples 10 minutes prior to analysis. BD LSRFortessa flow cytometer equipped with 355, 405, 488, 561 and 640 nm lasers and DIVA software (BD Biosciences) was used to record 100,000 events per sample. Live gate, light scatter gate, doublet discrimination gate, and fluorescent gates CD45, CD31, CD55 and CD34 set according to fluorescence minus one -controls were applied and the data analysis was performed with FlowJo Software v10.8.0 (BD Biosciences).

RNA isolation, cDNA synthesis and real-time qPCR

Total RNA was purified using the NucleoSpin RNA kit [#740955, Macherey-Nagel] and the concentration and purity of the samples were measured using a NanoDrop 2000 spectrophotometer [Thermo Fisher Scientific]. Reverse transcription and mRNA levels were performed/analyzed with iScript cDNA synthesis [#1708891, BioRad] and iQ SYBR® Green Supermix [#1708882, BioRad] kits, respectively. Relative expression levels were calculated with the comparative Ct-method: $2^{\Delta Ct\text{-target gene}}/2^{\Delta Ct\text{-reference gene}}$. The following primers were used: *TERT* (FW: 5'-GAG AAC AAG CTG TTT GCG GG-3'; RV: 5'-AAG TTC ACC ACG

CAG CCA TA-3'), *pac* (FW: 5'-GTC TGG GTA GTG CCG TAG TG-3'; RV: 5'-ATT CCG TGG TGC GCT AGT TT-3'), *B2M* (FW: 5'-AAG GAC TGG TCT TTC TAT CTC-3'; RV: 5'-GAT CCC ACT TAA CTA TCT TGG-3'), *PDK4* (FW: 5'- CTA CTG GAC TTT GGT TCA GAA A-3'; RV: 5'- GCA CTG AAG AGG TAT TTA CTA ATT G-3') and *18S* (FW: 5'-TGA CTC AAC ACG GGA AAC C-3'; RV: 5'-TCG CTC CAC CAA CTA AGA AC-3').

Western blot analyses

Cells were lysed in RIPA buffer [#89901, Thermo Fisher Scientific] supplemented with 1x protease inhibitor cocktail [#11836170001, Merck] as well as 1x phosphatase inhibitors [#4906837001, Merck]. Protein concentrations were determined using the Pierce BCA kit [#655101, Greiner-bio One]. Twenty µg aliquots of total protein were mixed with Laemmli buffer and heated at 95° C for five minutes. Proteins were separated by SDS–PAGE and transferred to PVDF membranes [Transblot turbo kit #1704274, BioRad]. Membranes were incubated in blocking solution (3% of ECL blocking agent [#RPN418, GE Healthcare] in Tris-buffered saline supplemented with 0.1% Tween 20 (TBST)) for one hour at room temperature and subsequently in blocking solution supplemented with primary antibody (anti-telomerase reverse transcriptase [1:1000, #ab32020, Abcam] and anti-GAPDH [1:1000, #2118, Cell Signaling]) overnight at 4°C. After several washes in TBST, membranes were incubated in blocking solution supplemented with horseradish peroxidase-conjugated mouse anti-rabbit secondary antibody [1:10000, #7074S, Cell Signaling] for one hour at room temperature, washed several times in TBST, and incubated with ECL western-blotting detection reagent [#12644055, Thermo Fisher Scientific]. Images were acquired using the ChemiDoc MP Imaging System (Bio-Rad Laboratories).

Adiponectin secretion

Conditional media from cells, before and after differentiation, were collected three days after the last media change to determine adiponectin secretion by ELISA following the protocol provided by the manufacturer [#DRP300, R&D systems].

Basal and stimulated lipolysis

Cells were incubated in lipolysis medium (phenol red-free DMEM/F12 [#7074S, Gibco] supplemented with 2% BSA [#A4503, Sigma-Aldrich]) without (basal) or with isoprenaline [#I5627, Sigma-Aldrich], dibutyryl-cAMP [#D0627, Sigma-Aldrich], TNF-α [#T7539, Sigma-Aldrich] or insulin [#I9278, Sigma-Aldrich] in combination with 8-Bromoadenosine 3′,5′-cyclic monophosphate sodium salt [#B7880, Sigma-Aldrich] for three hours at 37°C. Glycerol release into the culture media was subsequently quantified to determine basal and stimulated lipolysis as described previously (26).

Lipogenesis assay

Cells were cultured as described above with the following modifications: **i)** at day 11 of differentiation, insulin was removed from the media, **ii)** at day 13, cells were incubated in DMEM without glucose [#F0405 Biochrom AG, Merk] and **iii)** at day 14, cells were incubated in glucose-free DMEM supplemented with 1 µM glucose for three hours [#A24940, Thermo Fisher Scientific]. Subsequently, cells were culture in glucose-free DMEM supplemented with 0.125 mCi [3-^{3}H]-D-glucose [#NET331A001MC, PerkinElmer] and 1 µM glucose DMEM with or without insulin [#I9278, Sigma-Aldrich] for three hours. Prior to lysis in H_2O supplemented with 0.1% SDS [#I4509, Sigma-Aldrich], cells were washed three times in cold PBS. One part of the lysate was used to determine protein concentration using the BCA Protein determination kit and the other part the lysate was added to scintillation liquid (Optiphase HiSafe 3 scint solution [#1200.437, PerkinElmer]) and counting per minute (CPM) was measured using a β-counter [Trib Carb 4910 TR, PerkinElmer] using the QuantaSmart software.

Proteomics

Proteomics sample preparation

Samples for proteome measurement were prepared using the inStageTip (iST) method (27). In detail, frozen samples were mixed with SDC buffer (100 mM Tris-HCl, pH 7.6, and 2% (w/v) SDC) to a final concentration of 1% SDC, heated (five minutes, 95°C) and sonicated (Diagenode Bioruptor, high intensity, 15 x 30 seconds). After determining protein concentration by BCA assay, 30 µg protein were reduced and alkylated using 10 mM TCEP and 40 mM CAA (five minutes, 40°C in the dark). Samples were digested with trypsin and LysC (1:50 protein:enzyme) overnight at 37°C. Peptides were acidified with TFA (1% final concentration) and loaded onto activated triple layer styrenedivinylbenzene–reversed phase sulfonated STAGE tips (SDB-RPS; 3M Empore) and washed with 100 µl ethylacetate 1% TFA, 100µl 30% methanol 1% TFA and 150 µl 0.2% TFA. Peptides were eluted with 60 µl SDB-RPS elution buffer (80% ACN, 5% NH_4OH), followed by evaporation of the solution in a SpeedVac for 40 minutes at 45°C. Desalted peptides were re-solved in 10 µl MS loading buffer (2% ACN, 0.1% TFA) and stored at -20°C until measurement.

LC-MS/MS analysis

Proteomes were measured using a 115 minute long single-shot data-independent acquisition (DIA) method on an Orbitrap Exploris 480 mass spectrometer [Thermo Fisher Scientific]. For this, 500 ng of peptide mixture were separated on an in-house packed column (1.9 µm C18 ReproSil particles, Dr. Maisch GmbH) using the EASY-nLC 1200 liquid chromatography unit [Thermo Fisher Scientific]. Peptides were separated on a binary buffer system consisting of buffer A and B (0.1% formic acid and 80% ACN, 0.1% formic acid, respectively) in which buffer B changed from 5% to 45% over the elution. Peptides were ionized via electrospray (ESI) and pre-filter b FAIMS [Thermo Fisher Scientific] switching between a constant voltage (CV) of -50V/-70V each corresponding to a full ms1/ms2 DIA cycle. The cycle consisted of a ms1 scan (300-1650 m/z, max. ion fill time of 45ms, normalized AGC target = 300%, R= 120.000 at 200 m/z) followed by 49 tMS2 fragment scans of unequally spaced windows in

the same m/z range (fill time = 22 ms, normalized AGC target = 1000%, normalized HCD collision energy = 30%, R= 15.000).

Bioinformatic workflow and data analysis

The DIA raw files were processed using Spectronauts (v14.9.201124.47784) directDIA function (28) with default settings. Spectra were searched against a human UniProt regular and “additional “FASTA database (UP000005640_9606_2020-06; 20,609 and 77,157 entries respectively) and filtered for contaminants (MaxQuant contaminants list, 245 entries). Spectronaut report files were further analyzed with Perseus (v.1.6.14.0).

Transcriptomics

Total RNA from hAPCs (P12) and TERT-hAPCs (P52) was subjected to quality control with Tapestation (Agilent) according to the manufacturer’s instructions. To construct libraries suitable for Illumina sequencing, the stranded mRNA sample preparation protocol was used with starting concentration between 25-1000 ng total RNA. The protocol includes mRNA isolation, cDNA synthesis, ligation of adapters and amplification of indexed libraries. Library yield and quality were analyzed using a Qubit (Thermo Fisher Scientific) and a Tapestation (Agilent), respectively. The indexed cDNA libraries were normalized and combined, and the pools were sequenced on the Illumina Nextseq 2000 P2 100 cycle sequencing run, generating 58 base paired end reads with dual index. Basecalling and demultiplexing was performed using Illumina bcl2fastq (v2.20). Sequence data quality was assessed using FastQC (v0.11.8). Reads were aligned to Ensembl GRCh38 reference genome using STAR (v2.6.1d). Gene counts were estimated using featureCounts (v1.5.1). Count data was imported to Bioconductor package limma-Voom (v3.53.1) and tested for differential expression between different cell type. Gene set over-representation analysis for the significantly regulated genes at different comparison was performed using Enrichr function in ClusterProfiler package (v 4.4.2). The Hallmark gene set from MsigDB (Broad Institute) was used to calculate the enrichment.

Integration of proteomic and transcriptomic data

The transcriptomic and proteomic data were analyzed as described under the respective header. The resulting tables from these analyses were overlapped based on gene symbols and 4,700 genes were found to be present in both data sets. Out of these, 588 entries displayed congruent mRNA and protein regulation at a false discovery rate <0.05 comparing edited vs. non-edited adipocytes.

Imaging of 2D cell cultures

Cells were plated in 170 µm thick glass-bottom 96 or 24 well plates [#5242-20 or #5232-20, zell-kontakt] and cultured as described above. On day 13 of differentiation, cells were fixed in PBS supplemented with 4% paraformaldehyde [#SC281692, Santa Cruz Biotechnology] for ten minutes at room temperature and washed three times with PBS. Lipid droplets and nuclei were stained by incubating the cells for ten minutes at room temperature with PBS supplemented with BODIPY 493/503 [1:2500, #D3922, Thermo Fisher Scientific] and Hoechst 33342 [1:5000, #H21492, Invitrogen], respectively. Subsequently, cells were washed three times with PBS. Images were acquired using a Nikon Spinning disk CREST v3 inverted microscope with BSIexpress sCMOS camera (6.5um pixels) and using 20x/0.75 air and 60x/1.2 water objectives.

Imaging of 3D cell cultures

Spheroids were cultured as described above, fixed for one hour in PBS supplemented with 4% paraformaldehyde and stained with BODIPY 493/503 and DRAQ5 [1:1000, #65088092, Thermo Fisher Scientific]. Spheroids were mounted in 1.2% low melting point agarose in 170 µm thick glass-bottom 24 well plates [#5232-20, zell-kontakt] and cleared with the SeeBD method as previously described (4). Z-stacks were acquired using a Nikon Spinning disk CREST v3 inverted microscope with BSIexpress sCMOS camera using a 25x/1.05 silicone

objective and denoised using the NIS elements Denoise.Ai pre-trained algorithm. Representative images are displayed as maximum intensity projections.

Statistics and data availability

Upon acceptance of this work or reviewers' requests, transcriptomic and proteomic raw data will be available through the Gene Expression Omnibus repository and the Proteomics Identification Database, respectively. Results are expressed as mean ± SEM and statistical tests are indicated in the figure legends. Data analyses were performed using GraphPad Prism software (version 9.0, San Diego, CA) and statistical significance is indicated as: *p<0.05, **p<0.01, ***p<0.001, ****p<0.0001.

AUTHOR CONTRIBUTIONS

M.C., N.M., and M.R. wrote the first version of the manuscript, which was subsequently edited and approved by all co-authors. M.C. and T.D.C.B immortalized and functionally characterized the cells. H.G. and L.M. performed bioinformatic analyses. J.J. generated and analyzed FACS data. M.C., M.O-H and T.D.C.B imaged the cells. F.K. and N.K. generated proteomic results.

DECLARATION OF INTERESTS

None of the authors have any conflict of interest to report.

ACKNOWLEDGEMENTS

The pSpCas9(BB)-2A-GFP plasmid (PX458) was a gift from Dr. Feng Zhang. Parts of the study was performed at the Live Cell imaging Core facility/Nikon Center of Excellence, at the Karolinska Institute, supported by grants from the Swedish Research Council, KI infrastructure, and Centre for Innovative Medicine. For the image analysis, we acknowledge the help of Gisele Miranda at The BioImage Informatics Facility at SciLifeLab, National Microscopy Infrastructure (VR-RFI 2019-00217), and recipient of the Chan-Zuckerberg Initiative. We also acknowledge the help from the MedH Flow Cytometry core facility and the Bioinformatics and Expression Analysis (BEA) core facility, both of which are supported by the board of research at the Karolinska Institutet and the research committee at the Karolinska Hospital (Stockholm County Council).

This work was supported by grants from Margareta af Uggla's foundation (M.R.), the Swedish Research Council (M.R., N.M.), ERC-SyG SPHERES (856404 to M.R.), the NovoNordisk Foundation (including the Tripartite Immuno-metabolism Consortium Grant Number NNF15CC0018486, the MSAM consortium NNF15SA0018346 and the MeRIAD consortium Grant number 0064142, all three M.R. and NNF20OC0061149 to N.M.), Knut and Alice Wallenbergs Foundation (including Wallenberg Clinical Scholar to M.R.), CIMED (N.M.

and M.R.), the Swedish Diabetes Foundation (M.R.), the Stockholm County Council (M.R.), the Strategic Research Program in Diabetes at Karolinska Institutet (M.R., H.G.), and the European Foundation for the Study of Diabetes (Future Leaders awards to N.M. and N.K.).

DATA AVAILABILITY STATEMENT

The data that support the findings of this study are available on request from the corresponding author; MR. The data are not publicly available due to their containing information that could compromise the privacy of research participants.

AUTHORS INFORMATION AND ORCID

Morgane Couchet morgane.couchet@cea.fr
Hui Gao hui.gao@ki.se
Felix Klingelhuber felix.klingelhuber@helmholtz-muenchen.de
Jutta Jalkanen jutta.jalkanen@ki.se
Thais De Castro Barbosa thais.de-castro-barbosa@ki.se
Muhmmad Omar-Hmeadi omar.hmeadi@ki.se>
Lucas Massier lucas.massier@ki.se
Natalie Krahmer natalie.krahmer@helmholtz-muenchen.de
Niklas Mejhert niklas.mejhert@ki.se ORCID 0000-0003-1785-833X
Mikael Rydèn mikael.ryden@ki.se, ORCID 0000-0003-4785-1876

REFERENCES

1. Sakers A, De Siqueira MK, Seale P, Villanueva CJ. Adipose-tissue plasticity in health and disease. Cell. 2022;185(3):419- 46.
2. Dufau J, Shen JX, Couchet M, De Castro Barbosa T, Mejhert N, Massier L, et al. In vitro and ex vivo models of adipocytes. Am J Physiol Cell Physiol. 2021;320(5):C822-41.
3. Hu W, Lazar MA. Modelling metabolic diseases and drug response using stem cells and organoids. Nat Rev Endocrinol. 2022;18(12):744-59.
4. Shen JX, Couchet M, Dufau J, de Castro Barbosa T, Ulbrich MH, Helmstädter M, et al. 3D Adipose Tissue Culture Links the Organotypic Microenvironment to Improved Adipogenesis. Adv Sci Weinh Baden-Wurtt Ger. 2021;8(16):e2100106.
5. Klingelhutz AJ, Gourronc FA, Chaly A, Wadkins DA, Burand AJ, Markan KR, et al. Scaffold-free generation of uniform adipose spheroids for metabolism research and drug discovery. Sci Rep. 2018;8(1):523.
6. Ioannidou A, Alatar S, Schipper R, Baganha F, Åhlander M, Hornell A, et al. Hypertrophied human adipocyte spheroids as in vitro model of weight gain and adipose tissue dysfunction. J Physiol. 2022;600(4):869-83.
7. Markussen LK, Isidor MS, Breining P, Andersen ES, Rasmussen NE, Petersen LI, et al. Characterization of immortalized human brown and white pre-adipocyte cell models from a single donor. PloS One. 2017;12(9):e0185624.
8. Masnikov D, Stafeev I, Michurina S, Zubkova E, Mamontova E, Ratner E, et al. hTERT-immortalized adipose-derived stem cell line ASC52Telo demonstrates limited potential for adipose biology research. Anal Biochem. 2021;628:114268.
9. Shamsi F, Tseng YH. Protocols for Generation of Immortalized Human Brown and White Preadipocyte Cell Lines. Methods Mol Biol Clifton NJ. 2017;1566:77-85.
10. Wang L, Song K, Qu X, Wang H, Zhu H, Xu X, et al. hTERT gene immortalized human adipose-derived stem cells and its multiple differentiations: a preliminary investigation. Appl Biochem Biotechnol. 2013;169(5):1546-56.
11. Wolbank S, Stadler G, Peterbauer A, Gillich A, Karbiener M, Streubel B, et al. Telomerase immortalized human amnion- and adipose-derived mesenchymal stem cells: maintenance of differentiation and immunomodulatory characteristics. Tissue Eng Part A. 2009;15(7):1843-54.
12. Tyurin-Kuzmin PA, Chechekhin VI, Ivanova AM, Dyikanov DT, Sysoeva VY, Kalinina NI, et al. Noradrenaline Sensitivity Is Severely Impaired in Immortalized Adipose-Derived Mesenchymal Stem Cell Line. Int J Mol Sci. 2018;19(12):3712.
13. Ran FA, Hsu PD, Wright J, Agarwala V, Scott DA, Zhang F. Genome engineering using the CRISPR-Cas9 system. Nat Protoc. 2013;8(11):2281-308.
14. Hellmér J, Arner P, Lundin A. Automatic luminometric kinetic assay of glycerol for lipolysis studies. Anal Biochem. 1989;177(1):132-7.
15. Massier L, Jalkanen J, Elmastas M, Zhong J, Wang T, Nono Nankam PA, et al. An integrated single cell and spatial transcriptomic map of human white adipose tissue. Nat Commun. 2023;14(1):1438.
16. Kulak NA, Pichler G, Paron I, Nagaraj N, Mann M. Minimal, encapsulated proteomic-sample processing applied to copy-number estimation in eukaryotic cells. Nat Methods. 2014;11(3):319-24.
17. Bekker-Jensen DB, Bernhardt OM, Hogrebe A, Martinez-Val A, Verbeke L, Gandhi T, et al. Rapid and site-specific deep phosphoproteome profiling by data-independent acquisition without the need for spectral libraries. Nat Commun. 2020;11(1):787.

18. Schwalie PC, Dong H, Zachara M, Russeil J, Alpern D, Akchiche N, et al. A stromal cell population that inhibits adipogenesis in mammalian fat depots. Nature. 2018;559(7712):103-8.
19. Dong H, Sun W, Shen Y, Baláz M, Balázová L, Ding L, et al. Identification of a regulatory pathway inhibiting adipogenesis via RSPO2. Nat Metab. 2022;4(1):90-105.
20. Rennert RC, Januszyk M, Sorkin M, Rodrigues M, Maan ZN, Duscher D, et al. Microfluidic single-cell transcriptional analysis rationally identifies novel surface marker profiles to enhance cell-based therapies. Nat Commun. 2016;7:11945.
21. Lin CS, Ning H, Lin G, Lue TF. Is CD34 truly a negative marker for mesenchymal stromal cells? Cytotherapy. 2012;14(10):1159-63.
22. Ryden M, Dicker A, van Harmelen V, Hauner H, Brunnberg M, Perbeck L, et al. Mapping of early signaling events in tumor necrosis factor-alpha -mediated lipolysis in human fat cells. J Biol Chem. 2002;277(2):1085-91.
23. Maqsood MI, Matin MM, Bahrami AR, Ghasroldasht MM. Immortality of cell lines: challenges and advantages of establishment. Cell Biol Int. 2013;37(10):1038-45.
24. Kotin RM, Linden RM, Berns KI. Characterization of a preferred site on human chromosome 19q for integration of adeno-associated virus DNA by non-homologous recombination. EMBO J. 1992;11(13):5071-8.
25. Smith JR, Maguire S, Davis LA, Alexander M, Yang F, Chandran S, et al. Robust, persistent transgene expression in human embryonic stem cells is achieved with AAVS1-targeted integration. Stem Cells Dayt Ohio. 2008;26(2):496-504.
26. Buechler MB, Pradhan RN, Krishnamurty AT, Cox C, Calviello AK, Wang AW, et al. Cross-tissue organization of the fibroblast lineage. Nature. 2021;593(7860):575-9.
27. Hepler C, Shan B, Zhang Q, Henry GH, Shao M, Vishvanath L, et al. Identification of functionally distinct fibro-inflammatory and adipogenic stromal subpopulations in visceral adipose tissue of adult mice. eLife. 2018;7:e39636.
28. Shao M, Vishvanath L, Busbuso NC, Hepler C, Shan B, Sharma AX, et al. De novo adipocyte differentiation from Pdgfrβ+ preadipocytes protects against pathologic visceral adipose expansion in obesity. Nat Commun. 2018;9(1):890.

FIGURE LEGENDS

Figure 1: Targeted knock in of TERT-hAPCs results in cells with improved proliferative capacity.

A) Overview of the AAVS1 safe harbor *PPP1R12C* locus, including the T2 guide targeting site.

B) Strategy for establishing TERT-hAPCs using dual selection steps.

C) Messenger RNA levels of *TERT* and *pac* gene in both WT- and TERT-hAPCs (n=4). N.d.=not detectable.

D) TERT protein quantification in WT- and TERT-hAPCs (n=3).

E) Cumulative numbers of WT- and TERT-hAPCs over multiple passages.

F) Representative picture of WT- (P19) and TERT-APCs (P65) in the proliferative state.

G) Comparison of doubling times between WT- (25.4h, n=14) and TERT-hAPCs (20.8h, n=17). Statistical differences were determined by Mann-Whitney U test.

H) Quantification of selected cell surface markers in WT- and TERT-hAPCs in the indicated passages by flow cytometry (data from one representative run are shown).

Figure 2: WT- and TERT-hAPCs display high adipogenic capacities.

A) Representative images of WT- and TERT-hAPCs at the indicated passages. Scale bars, 50 µm and 20 µm (inlay).

B) Adiponectin levels in conditioned media in undifferentiated (ctrl) and differentiated of WT- and TERT-hAPCs.

C) Pathway analysis of genes/proteins up- or down-regulated in TERT- *vs.* WT-hAPCs. EMT= epithelial-to-mesenchymal transition.

Figure 3: TERT-hAPCs display lipid handling characteristics similar to WT-APCs.

A-C) Lipolysis induced for three hours by the non-selective beta-adrenergic receptor agonist isoprenaline (A), the phosphodiesterase-resistant cAMP analogue dcAMP (B) and TNF-α

(C). Statistical differences were determined by two-way ANOVA followed by a Sidak post-hoc test.

D) Basal and insulin-stimulated lipogenesis was quantified in WT- and TERT-hAPCs. In panels A-D , WT-APCs were used at passage 15 and TERT-hAPCs at passage 50. **E)** Glycerol release following incubation without or with insulin at indicated concentrations expressed as fold-change over 8-bromo cAMP-stimulated lipolysis. **F)** *PDK4* mRNA levels determined by qPCR in WT-APCs (passage 15) and TERT-hAPCs (passage 32) incubated without or with insulin at the indicated concentration. Statistical differences were determined by two-way ANOVA followed by a Sidak post-hoc test. *= $P<0.05$, **= $P<0.01$, ***= $P<0.001$, ****=$P<0.0001$

Figure 4: TERT-APCs differentiate into adipocytes in 3D cultures.

A) Representative images of WT- and TERT-hAPC spheroids. Results are presented as maximum intensity projections from Z-stacks of images. Scale bars, 50 µm and 20 (inlay).

B) Both WT- and TERT-hAPCs 3D-spheoroids respond to isoprenaline-stimulated lipolysis (n=4). Statistical differences were determined by one-way ANOVA followed by a Tukey's post-hoc test. WT- and TERT-hAPCs were used at passage 15 and 50, respectively. ****=$P<0.0001$

Supplementary Figure S1: TERT-hAPCs maintain lipid accumulation in late passages.

Representative images of **A)** TERT-hAPCs at passage 84, **B)** ASC52telo at passage 38 and **C)** TERT-hWA at passage 37. For panel A scale bars are 50 µm and 20 µm for inlays, for panels B-C scale bars are 20 µm and 10 µm for inlays.

Supplementary Figure S2: TERT-hAPCs maintain insulin sensitivity in late passages.

Experiments in TERT-hAPCs at passage 82 show **A)** glycerol release following incubation without or with insulin at indicated concentrations expressed as fold-change over 8-bromo cAMP-stimulated lipolysis, **B)** *PDK4* mRNA levels determined by qPCR following incubation

without or with insulin. Statistical differences were determined by one-way ANOVA followed by Tukey's post-hoc test (panel A) or Student's unpaired t-test (panel B). *= $P<0.05$, **= $P<0.01$, ****=$P<0.0001$

Figure 1

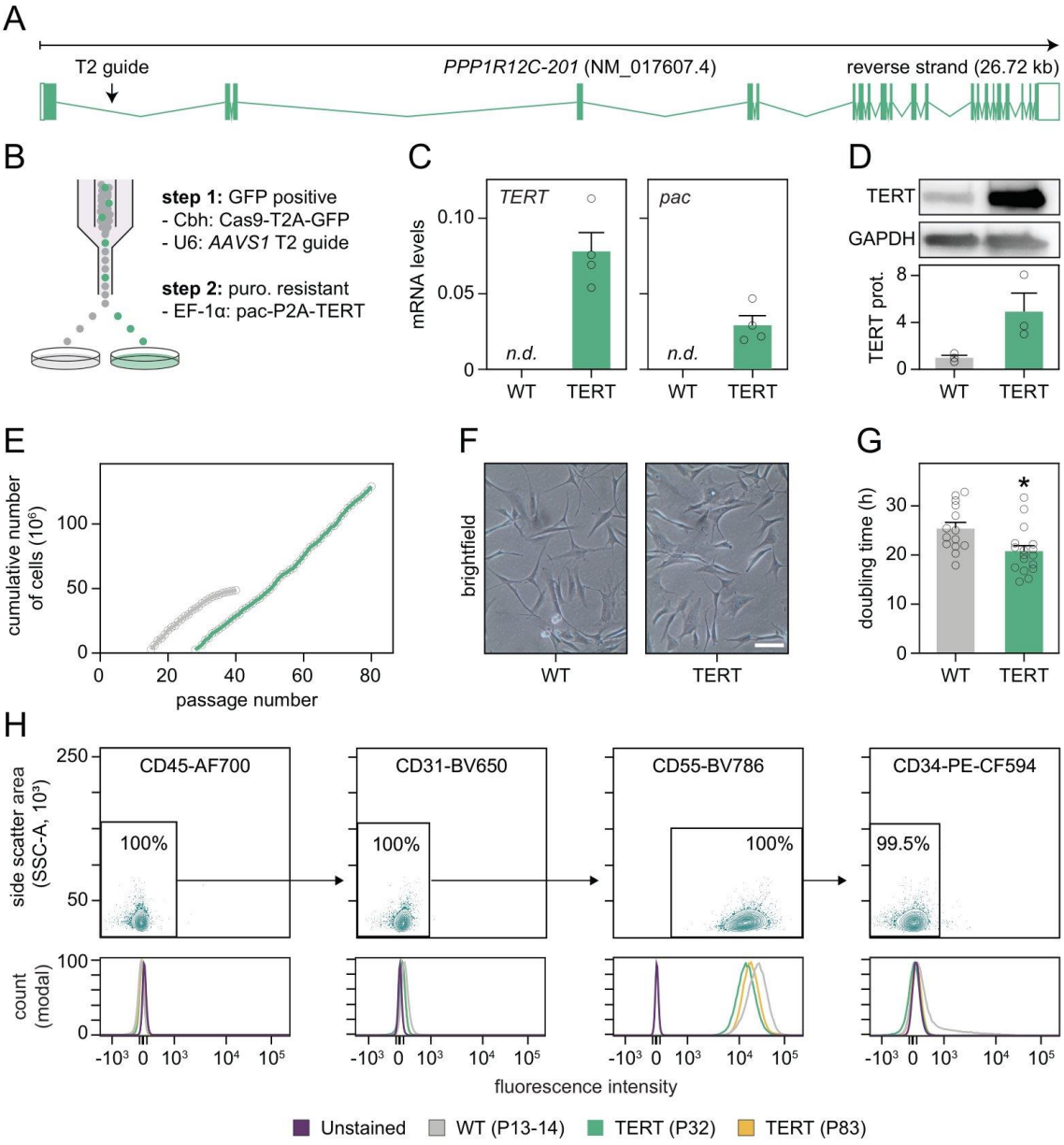
A
T2 guide
PPP1R12C-201 (NM_017607.4)
reverse strand (26.72 kb)
B
step 1: GFP positive
- Cbh: Cas9-T2A-GFP
- U6: AAVS1 T2 guide
step 2: puro. resistant
- EF-1α: pac-P2A-TERT
C
TERT
pac
mRNA levels
n.d.
n.d.
WT
TERT
D
TERT
GAPDH
TERT prot.
E
cumulative number of cells (10⁶)
passage number
F
brightfield
G
doubling time (h)
H
CD45-AF700
CD31-BV650
CD55-BV786
CD34-PE-CF594
100%
99.5%
side scatter area (SSC-A, 10³)
count (modal)
fluorescence intensity
Unstained
WT (P13-14)
TERT (P32)
TERT (P83)

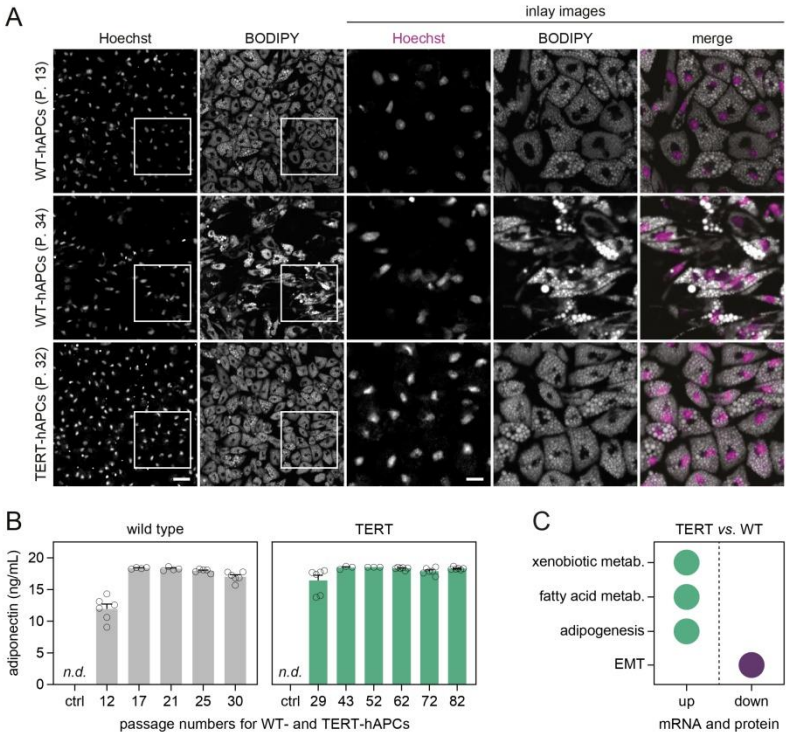

Figure 2

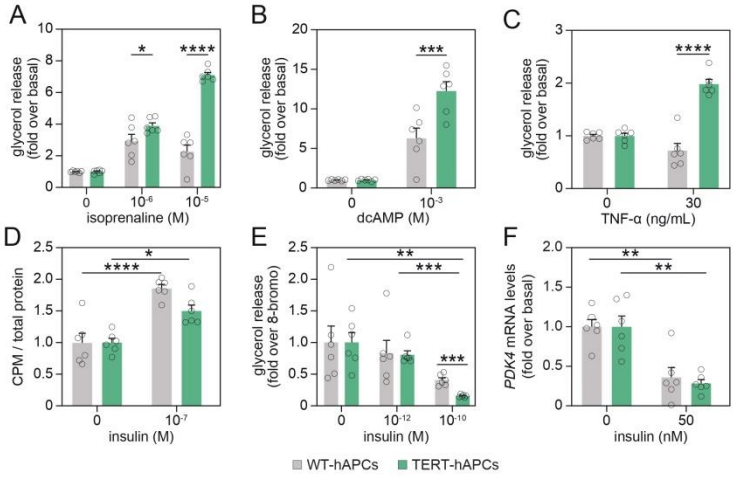

Figure 3

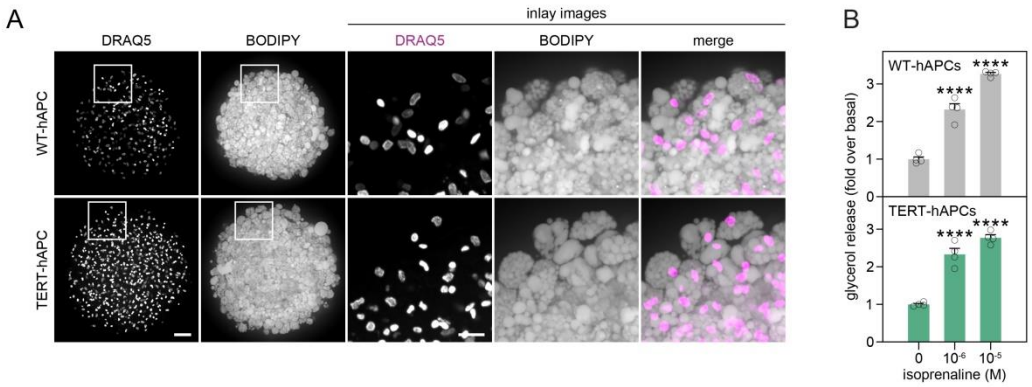

Figure 4